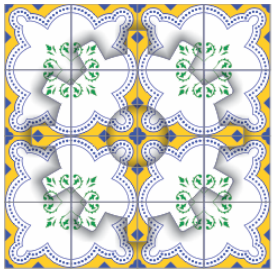

CONEM 2012 «Engenharia em destaque»
VII Congresso Nacional de Engenharia Mecânica
São Luís - Maranhão - Brasil
31 de julho a 03 de agosto
www.abcm.org.br/conem2012

A FINITE ELEMENT FOR ACTIVE COMPOSITE PLATES WITH PIEZOELECTRIC LAYERS APPLIED TO COMPOSITE CYLINDERS

Murilo Sartorato, murilosart@gmail.com[1]
Ricardo de Medeiros, medeiros@sc.usp.br[1]
Marcelo Leite Ribeiro, strova@hotmail.com[1]
Volnei Tita, voltita@sc.usp.br[1]

[1] USP – Universidade de São Paulo, EESC – Escola de Engenharia de São Carlos – Av. Trabalhador São Carlense, 400 – 13 São Carlos /SP, Brasil

Abstract. *In recent years, the study of smart composite materials has increased due to the development of active piezoelectric fibers that can be produced into thin patches of laminates made of piezoelectric fibers reinforced polymers that, unlike the more common used piezoceramics, can undergo large displacements and strains without fracturing. This characteristic improves the potential of such materials as curved shaped laminates can be produced and used as both sensors and actuators in non-planar structures for several applications such as structure health monitoring, damage identification, vibration control and/or suppression, energy harvesting, along with others. However, several obstacles remain to the practical application of this technology: difficulty in fiber manufacturing techniques, mechanical and electrical properties prediction and obtainment and mechanical behavior prediction and simulation. In this work, a model for structural composite laminates containing active piezoelectric layers is presented and used to formulate a shell quadratic finite element with eight nodes for large displacements and curved structures. The element was implemented into the finite element commercial package Abaqus through its UEL (User ELement) Fortran subroutine. Numerical results of carbon-epoxy composite cylinders with macro-fiber composites (MFC) piezoelectric patches attached under static and/or dynamic load cases are presented.*

Keywords: *finite elements, smart materials, composite materials*

1. INTRODUCTION

In the last decades, the use of piezoelectric smart composite material in both academic and industrial environments has been steadily increasing, especially in areas that focus on highly optimized structural projects, such as the aeronautical, aerospace and petroleum industries. In particular, in the aeronautic industry, smart structures features of having embedded sensors and actuators can lead to great improvements on an aeronautic structure performance by using practices like: structure health monitoring, flow-control, vibration control, flutter control and energy harvesting.

However, the use of the common piezoelectric ceramics introduces limitations in both the production and usage of smart structures due to its brittleness, large dimensions thick-wise, and low flexibility. In the last years, the development of piezoelectric materials in the form of fibers solved some of these limitations. The concept of piezoelectric fibers allowed the creation of laminated composite materials with active fiber embedded in polymer matrixes, creating smart composite materials that have high flexibility, structural resistance and can be applied to curved surfaces.

Still, several obstacles remain to the practical application of this technology: difficulty in fiber manufacturing techniques, mechanical and electrical properties prediction and obtainment and mechanical behavior prediction and simulation.

Several works have been published in the last years about the simulation of such structures using finite elements. Some researchers like Paik et al (2007) defend that simpler models cannot completely simulate a smart composite, and simulations must be made using a micro-scale modeling of each fiber. This approach comes with a great computational cost and is impractical for large structures. As such, several researchers implement plate finite element models that simulate smart composites, in particular, Azzouz et al (2001), Gabbert et al (2004) and Marinković et al (2008) presented linear plate finite element models for active composites with increasing complexity theories. In this work, a finite element model for active fiber composites is proposed.

However, as noted by Azzouz et al (2001) and Marinković et al (2008), the great flexibility introduced by the polymer matrixes in the fibers and the electro-mechanic coupling makes the non-linear behavior of great rotations prominent in some cases.

As such, in this work, a non-linear plate finite element for smart composites is proposed, using the von Karman deformations. Also, a co-rotational approach is used to both correctly simulate curved surfaces and link the electric-mechanical coupling equations to the Classical Theory of Laminates recovering the classic constitutive composite equations – the ABBD matrix.

The element was implemented into the finite element commercial package Abaqus through its UEL (User Element) Fortran subroutine. The advantage of the implementation of the models into pre-processing software like ABAQUS is the ability to easily model complex structures. The UEL subroutine affects only the element processing, specifically the residue and stiffness and mass matrixes calculations, as shown by Figure 1. As such, other phases of finite element analysis that are time consuming and difficult to program for complex structures like meshing, applying loads and boundary conditions and global matrixes assemble are covered by ABAQUS' functions and user interface.

Comparative results with works found on the literature of quasi-static analysis of composite plates and cylinders with piezoelectric patches are presented.

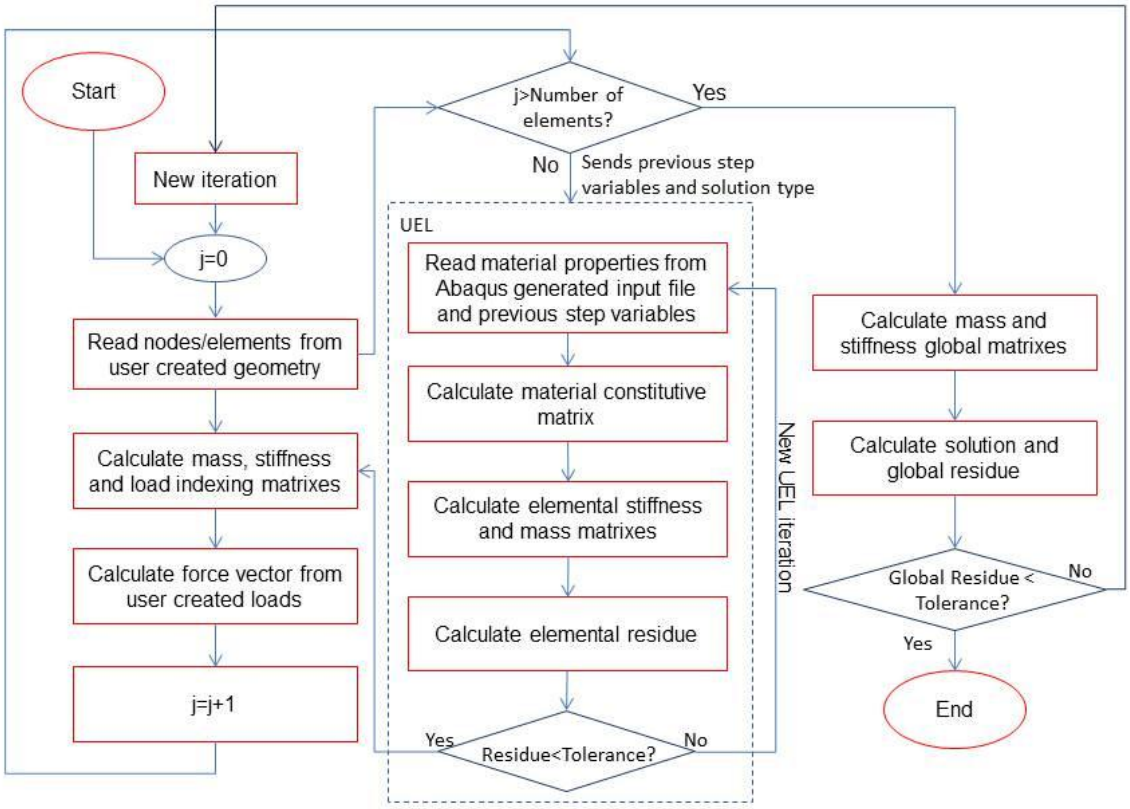

Figure 1. Summary of the Abaqus and UEL subroutine interactions

2. FORMULATION OF THE ELEMENT

In this section the constitutive equations for a piezoelectric active layer of composites, the composite layer-up equations and the kinematics and electrical assumptions used are presented. The constitutive equations for an piezoelectric active layer are based upon the works of Marinković et al (2007). The kinematic assumptions are modeled from the Reissner-Mindlin First-Order Shear Theory taken the adaptations for a co-rotational system made by Reddy and Ochoa (1996) and Gabbert (2004), which were based in the work of Ahmad et al (1970), extending the modeling with the use of von Kármán's non-linear deformation for small strains and great rotations. This was made as researchers such as Azzouz et al (2001) and Marinković et al (2008) noted that for some cases, the non-linear contribution of the displacements to the off-plane distortions (γ_{23} and γ_{13}) are prominent, which in turn are one of the main forms of piezoelectric effects coupling. Electrical assumptions are made based on Maxwell Equations and are discussed below.

2.1. Kinematic Assumptions

The classic kinematic equations for the displacements of a curved plate can be written in a co-rotational model by using three different coordinate systems: the natural system (ξ_1, ξ_2, ξ_3), the global system (x_1, x_2, x_3), and the co-rotational system (x_1', x_2', x_3'), shown in Figure 2. The co-rotational system (or local-running system) varies from node to

node where, the x_1' and x_2' axis are given by the normalized vectors that defines the tangent plane of the plate's mid-surface in a given node, and the x_3' axis is the normalized normal vector to this plane.

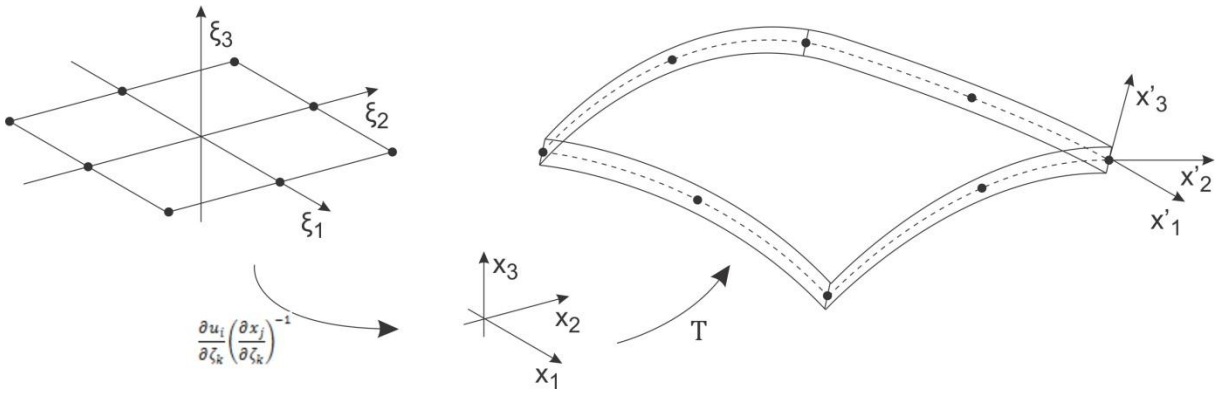

Figure 2. Coordinate systems used in the formulation

The First-Order Shear Theory uses Reissner-Mindlin assumptions for the plate displacements: any thickness direction line of a shell remains straight after deformation, but not necessarily normal to the mid-surface. As such, in the co-rotational system, the displacement of any point can be given by a sum of the displacements at the mid-surface $(u_1'^0, u_2'^0, u_3'^0)$ and a linear function on the rotations about the x_1' and x_2' axis (θ_1', θ_2'):

$$\boldsymbol{u} = \begin{Bmatrix} u_1' \\ u_2' \\ u_3' \end{Bmatrix} = \begin{Bmatrix} u_1^{0\prime} \\ u_2^{0\prime} \\ u_3^{0\prime} \end{Bmatrix} + x_3' \begin{Bmatrix} \theta_1' \\ \theta_2' \end{Bmatrix} \tag{1}$$

Equation (1) can be used in a discretized form with the shape functions ϕ_i and the degenerated coordinate transformation matrix H_i.

$$\boldsymbol{u} = \sum_{i=0}^{n} \phi_i(\xi_1, \xi_2) \begin{Bmatrix} u_1^{0\prime} \\ u_2^{0\prime} \\ u_3^{0\prime} \end{Bmatrix} + \zeta_3 \left(\frac{h_i}{2}\right) \phi_i(\xi_1, \xi_2) H_i \begin{Bmatrix} \theta_1' \\ \theta_2' \end{Bmatrix} \tag{2}$$

$$T_i = \begin{Bmatrix} e_1' \\ e_2' \\ e_3' \end{Bmatrix} = \begin{bmatrix} x_{1,\xi_1 i} & x_{2,\xi_1 i} & x_{3,\xi_1 i} \\ x_{1,\xi_2 i} & x_{2,\xi_2 i} & x_{3,\xi_2 i} \\ & e_1' \times e_2' & \end{bmatrix}, \; H_i = \begin{Bmatrix} -T_{i_2} \\ T_{i_1} \end{Bmatrix}^T, \; T_{R_i} = \begin{Bmatrix} T_{i_1} \\ T_{i_2} \end{Bmatrix} \tag{3}$$

It should be noted that the First-Order Shear Theory applies to the co-rotational system, and in this coordinate system there are five degrees of freedom associated with each node $(u_1'^0, u_2'^0, u_3'^0, \theta_1'^0, \theta_2'^0)$. A coordinate transformation using the coordinate transformation matrixes T and its degenerated counterparts for the rotations degree of freedom H and T_R, given by Eq. (3), can be applied recovering the six global degrees of freedom $(u_1^0, u_2^0, u_3^0, \theta_1, \theta_2, \theta_3)$, shown in Eq. (4).

$$\boldsymbol{u} = \sum_{i=0}^{n} \phi_i(\zeta_1, \zeta_2) T_i^T \begin{Bmatrix} u_{1_i}^0 \\ u_{2_i}^0 \\ u_{3_i}^0 \end{Bmatrix} + \zeta_3 \left(\frac{h_i}{2}\right) \phi_i(\xi_1, \xi_2) H_i T_{R_i}^T \begin{Bmatrix} \theta_1 \\ \theta_2 \\ \theta_3 \end{Bmatrix} \tag{4}$$

The constitutive equations, in special the stress-strain relations, presented in Eq. (16), are based in the co-rotational system of coordinates. As such the strain fields need to be calculated in the co-rotational system and are dependent on the displacement gradients. These gradients can be calculated in the global system of coordinates and transformed using the T matrix, as shown in Eq. (5).

$$\frac{\partial u_i'}{\partial x_j'} = T_{ki} \frac{\partial u_k}{\partial x_l} T_{lj}, \qquad \frac{\partial u_i}{\partial x_j} = \frac{\partial u_i}{\partial \zeta_k} \left(\frac{\partial x_j}{\partial \zeta_k}\right)^{-1} = \frac{\partial \phi_m}{\partial \zeta_k} \left(\frac{\partial \phi_n}{\partial \zeta_k}\right)^{-1} x_j^n u_i^m \tag{5}$$

Using the symmetric property of the strain tensor and the assumption of a plane state stress in each layer of the laminate, we can have the von Kármán strain vector given by:

$$\boldsymbol{\varepsilon}' = \begin{Bmatrix} \varepsilon'_{11} \\ \varepsilon'_{11} \\ \gamma'_{12} \\ \gamma'_{23} \\ \gamma'_{13} \end{Bmatrix} = \begin{Bmatrix} u'_{1,1} \\ u'_{2,2} \\ u'_{1,2} + u'_{2,1} \\ u'_{2,3} + u'_{3,2} \\ u'_{1,3} + u'_{3,1} \end{Bmatrix} + \frac{1}{2} \begin{Bmatrix} u^2_{3,1} \\ u^2_{3,2} \\ 2u'_{1,2}u'_{2,1} \\ 0 \\ 0 \end{Bmatrix} \tag{6}$$

Combining Eq. (5) and Eq. (6), the strain fields can be summarized as the following matrixes in Eq. (7).

$$\boldsymbol{\varepsilon}' = \left(\begin{bmatrix} B_m & \xi_3 B_f \\ B_{s_0} & B_{s_1} + \xi_3 B_{s_f} \end{bmatrix}^n + \begin{bmatrix} B_m u_i^n B_m + \xi_3 B_f \theta_i^n B_m & \xi_3 B_m u_i^n B_f \\ B_{s_0} u_i^n B_{s_0} + \xi_3 B_{s_1} \theta_i^n B_{s_0} & \xi_3 B_{s_0} u_i^n B_{s_1} \end{bmatrix} \right) \begin{Bmatrix} u_i \\ \theta_i \end{Bmatrix}^n \tag{7}$$
$$i = 1..3, n = number\ of\ nodes\ per\ element$$

Also, for a simpler formulation of the finite element, the B_u and $B_{u\varphi}$ matrixes can be defined:

$$B_u = \begin{bmatrix} B_m & 0 \\ 0 & B_f \\ B_{s_0} & B_{s_1} \\ 0 & B_{s_f} \end{bmatrix}^n + \begin{bmatrix} B_m u_i^n B_f & B_m u_i^n B_f \\ 0 & B_f \theta_i^n B_m \\ B_{s_0} u_i^n B_{s_0} & B_{s_1} \theta_i^n B_{s_0} \\ 0 & B_{s_0} u_i^n B_{s_1} \end{bmatrix}^n \tag{8}$$

$$B_{u\varphi} = \begin{bmatrix} B_m & 0 \\ 0 & B_f \end{bmatrix}^n + \begin{bmatrix} B_m u_i^n B_f & 0 \\ 0 & B_m u_i^n B_f + B_f \theta_i^n B_m \end{bmatrix}^n \tag{9}$$

It should be noted that in this formulation, the common used assumption for laminate composite plates that the in plane strains can be separated in a membrane contribution (ε_0) and a flexural contribution, linearly proportional to the curvature of the plate (κ_f) naturally appears. The same can be done with the off-plane distortions; they can be separated into a shearing portion (γ_0), related to the mid-surface displacements, and a torcional portion (γ_1 and κ_t) related to the rotations both directly (γ_1) and linearly (κ_t). These decompositions are given in Eq. (10).

$$\boldsymbol{\varepsilon}' = \begin{Bmatrix} \boldsymbol{\varepsilon} \\ \boldsymbol{\gamma} \end{Bmatrix} = \begin{Bmatrix} \boldsymbol{\varepsilon_0} \\ \boldsymbol{\gamma_0} + \boldsymbol{\gamma_1} \end{Bmatrix} + \xi_3 \begin{Bmatrix} \boldsymbol{\kappa_f} \\ \boldsymbol{\kappa_t} \end{Bmatrix} \tag{10}$$

The constant parts of the distortions are separated into γ_0 and γ_1 because each one is related to a different compatible external effort, as shown by Ahmad et al (1970).

2.2. Smart Composites Constitutive Equations

Problems with piezoelectric coupling are those in which an electric potential gradient causes deformation and vice-versa. There are different ways of writing the mechanical-electrical coupling (Ikeda, 1996), but for most problems and the formulation of finite element problems, in general, it is useful to use the e-form, which couples the mechanical stress fields with the electrical fields. This coupling between is characterized by the e_{kij} piezoelectric coefficients, and can be summarized by the tensorial relation in Eq. (11):

$$\begin{aligned} \sigma_{ij} &= C^E_{ijkl}\varepsilon_{kl} - e_{kij}E_k \\ D_i &= e_{ikl}\varepsilon_{kl} + d^{\varepsilon}_{ik}E_k \end{aligned}, \quad i,j,k,l = 1..3 \tag{11}$$

where: σ_{ij}, ε_{kl} and E_k are respectively: the stress, strain, and electrical fields; D_i are the components of the electrical displacements; C^E_{ijkl} is the fourth order elastic tensor for the short-circuit electrical bounding conditions ($E = constant$); d^{ε}_{ik} is the dielectric constants for a uniform displaced mechanical boundaries ($\varepsilon = constant$); and e_{ikl} are the piezoelectric coupling coefficients.

Due to the symmetry of the C, e and d tensors; the consideration that piezoelectric layers are transversely isotropic; and using the plane stress state ($\sigma_{33} = 0$) and uniaxial transversal polarization over the piezoelectric layers ($E_1 = E_2 = 0$) hypothesis, one can summarize Eq. (12).

$$\begin{Bmatrix}\sigma_{11}\\ \sigma_{22}\\ \sigma_{12}\\ -\\ \sigma_{23}\\ \sigma_{13}\\ -\\ D_3\end{Bmatrix}=\left[\begin{array}{ccc|ccc|c}Q_{11}&Q_{12}&0&0&0&e'_{31}\\ Q_{12}&Q_{11}&0&0&0&e'_{31}\\ 0&0&Q_{66}&0&0&0\\ \hline 0&0&0&Q_{44}&0&0\\ 0&0&0&0&Q_{44}&0\\ \hline e'_{31}&e'_{31}&0&0&0&-d'_{33}\end{array}\right]\begin{Bmatrix}\varepsilon_{11}\\ \varepsilon_{22}\\ \gamma_{12}\\ -\\ \gamma_{23}\\ \gamma_{13}\\ -\\ -E_3\end{Bmatrix}=\begin{bmatrix}Q_b&0&e^t\\ 0&Q_s&0\\ e&0&d\end{bmatrix}\begin{Bmatrix}\varepsilon_{11}\\ \varepsilon_{22}\\ \gamma_{12}\\ \gamma_{23}\\ \gamma_{13}\\ -E_3\end{Bmatrix} \tag{12}$$

Where:

$$Q_{11}=C_{11}^E-\frac{{C_{13}^E}^2}{C_{33}^E},\qquad Q_{12}=C_{12}^E-\frac{{C_{13}^E}^2}{C_{33}^E},\qquad Q_{44}=C_{44}^E+\frac{e_{15}^2}{d_{11}^\varepsilon},\qquad Q_{66}=2(C_{11}^E-C_{12}^E),\qquad e'_{31}=e_{31}-\frac{C_{13}^E}{C_{33}^E}e_{33},$$
$$d'_{33}=d_{33}^\varepsilon+\frac{e_{33}^2}{d_{11}^\varepsilon} \tag{13}$$

Starting from Eq. (12), one can use the Classical Laminated Theory to obtain the final constitutive equations for an active laminate. However, it should be noted that some changes to the theory must be applied: both the in-plane and off-plane matrixes Q_b and Q_s must be rotated in the angle of the fibers and the kinematic assumptions showed in Eq. (10) must be taken into account.

In particular, when the constitutive equation is integrated over the thickness, the effects of these kinematic assumptions creates more compatible generalized efforts over the laminate than the common used normal forces (N) and bending moments (B): the shear forces (Q) and torcional moments (T).

$$\begin{Bmatrix}Q_x\\ Q_y\end{Bmatrix}=\sum_{k=1}^{N}\int_{x'_{3k-1}}^{x'_{3k}}\begin{Bmatrix}\sigma_{23}\\ \sigma_{13}\end{Bmatrix}z\,dz \tag{14}$$

$$\begin{Bmatrix}T_x\\ T_y\end{Bmatrix}=\sum_{k=1}^{N}x'_3\int_{x'_{3k-1}}^{x'_{3k}}\begin{Bmatrix}\sigma_{23}\\ \sigma_{13}\end{Bmatrix}dz \tag{15}$$

As such, the classic ABBD laminate constitutive matrix is extended into the one shown in Eq. (18).

$$\begin{Bmatrix}N\\ M\\ Q\\ T\end{Bmatrix}=\begin{bmatrix}A&B&0&0\\ B&D&0&0\\ 0&0&G&G_h\\ 0&0&G_h&H\end{bmatrix}\begin{Bmatrix}\varepsilon_0\\ \kappa_f\\ \gamma_0+\gamma_1\\ \kappa_t\end{Bmatrix} \tag{16}$$

Where:

$$A_{ij}=\sum_{k=1}^{N}\overline{Q_{ij}^k}_b\left(x'_{3k}-x'_{3k-1}\right),\qquad B_{ij}=\frac{1}{2}\sum_{k=1}^{N}\overline{Q_{ij}^k}_b\left({x'_{3k}}^2-{x'_{3k-1}}^2\right),\qquad D_{ij}=\frac{1}{3}\sum_{k=1}^{N}\overline{Q_{ij}^k}_b\left({x'_{3k}}^3-{x'_{3k-1}}^3\right),$$
$$G_{ij}=\sum_{k=1}^{N}\overline{Q_{ij}^k}_s\left(x'_{3k}-x'_{3k-1}\right),\qquad G_{H_{ij}}=\frac{1}{2}\sum_{k=1}^{N}\overline{Q_{ij}^k}_s\left({x'_{3k}}^2-{x'_{3k-1}}^2\right),$$
$$H_{ij}=\frac{1}{3}\sum_{k=1}^{N}\overline{Q_{ij}^k}_s\left({x'_{3k}}^3-{x'_{3k-1}}^3\right) \tag{17}$$

Geometrically, we have that, given a plate in lateral view, γ_0 is related to the in-axis distortion, γ_1 is related to the section rotation due to torcional moments and, κ_t is related to the distortion of the section due to the torcional moments, as represented by Figure 3.

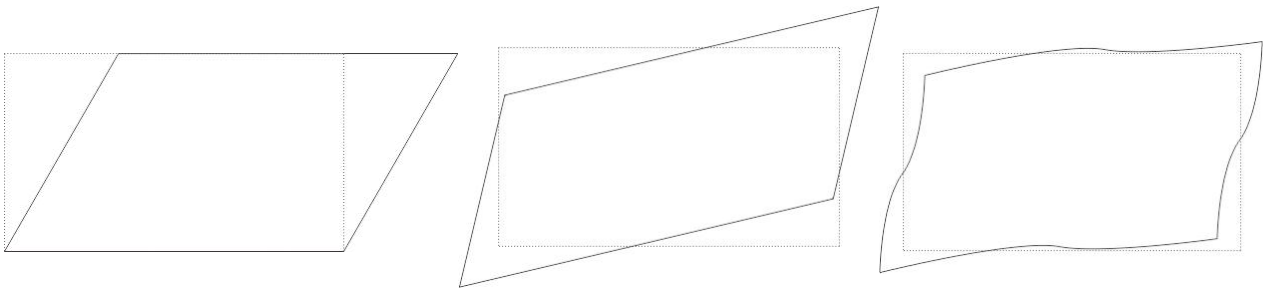

A **B** **C**

Figure 3. A. Geometric effect of γ_0 B. Geometric effect of γ_1 C. Geometric effect of κ_t

As the uniaxial transversal polarization over the piezoelectric layers ($E_1 = E_2 = 0$) hypothesis was used, there's no need for coordinate transformation of the fibers from layer to layer. This fact is enforced by the fact that in general, electrodes as installed over the plates, making the electrical fields always normal to each layer. This way, the integration of the dielectric and piezoelectric coupling parts of the constitutive matrix can be simplified to just a sum of the properties of each layer powdered by said layer thickness:

$$e'_{31_{laminate}} = \sum_{k=1}^{N} e'_{31_k} \left(x'_{3_k} - x'_{3_{k-1}}\right) \tag{18}$$

$$d'_{33_{laminate}} = \sum_{k=1}^{N} d'_{33_k} \left(x'_{3_k} - x'_{3_{k-1}}\right) \tag{19}$$

2.3. Electrical Assumptions

Starting from Gauss' Law, we have that:

$$\nabla \cdot D = \rho_f \tag{20}$$

As the electrodes of the laminates are usually installed such as there is only fields in the x'_3 direction, in this direction there is no free charge through the laminate thickness. Using this assumption with Eq. (12), we can write D_3 as a function of the strains and electric fields:

$$D_3 = e'_{31}(\varepsilon_{11} + \varepsilon_{22}) + d'_{33}E_3 \tag{21}$$

$$\frac{\partial D_3}{\partial x'_3} = e'_{31}\left(\frac{\partial \varepsilon_{11}}{\partial x'_3} + \frac{\partial \varepsilon_{22}}{\partial x'_3}\right) + d'_{33}\frac{\partial E_3}{\partial x'_3} = 0 \tag{22}$$

Using Eq. (22) with Faraday's Law of induction$E_3 = -\partial\varphi/\partial x'_3$, with the piezoelectric boundary conditions $\varphi\left(x'_1, x'_2, x'_3 = \frac{h}{2}\right) = \Delta\varphi$, $\varphi\left(x'_1, x'_2, x'_3 = -\frac{h}{2}\right) = 0$, we obtain the electrical field-difference of potential relation:

$$E_3 = -x'_3\frac{e'_{31}}{d'_{33}}\left(\frac{\partial \varepsilon_{11}}{\partial x'_3} + \frac{\partial \varepsilon_{22}}{\partial x'_3}\right) - \frac{\Delta\varphi}{h} \tag{23}$$

Therefore, the electrical field can be obtained from the difference of potential over the electrodes and the plate membrane strains gradient. This mechanical-electrical coupling in the electric fields is explained by the thickness reduction created by the Poisson effect, as Piefort (2000) said. However, as the term $\left(\frac{\partial \varepsilon_{11}}{\partial x'_3} + \frac{\partial \varepsilon_{22}}{\partial x'_3}\right)$ is usually difficult and computational expansive to be calculated. Also, this term is only relevant when compared to the difference of potential term in the specific application of the piezoelectric layer being used as a sensor in plates where its thickness is the greatest portion of the whole laminate – over 60% of the laminate total thickness according to Pieford (2000). That way, this term is ignored, and a discretized relation between the electric field and the difference of potential can be written:

$$E_3 = B_\varphi \varphi = -\frac{1}{h_i}\varphi_i \tag{24}$$

Where ϕ_i and h_i is, respectively, the difference of potential and the thickness over each node of the element.

3. FINITE ELEMENT EQUATIONS AND IMPLEMENTATION AS A UEL SUBROUTINE

As the final objective of the present work is to implement an active composite finite element in the Abaqus' UEL subroutine, only elemental quantities need to be calculated. In particular, the subroutine needs the internal forces vector and the non-linear equivalent of the mass, damping and stiffness matrixes. In the current model, both the mass and damping matrixes are considered constant, as the non-linear equivalent of the stiffness matrixes is the electric-mechanical enthalpy hessian matrix.

Given the energy potential over a single element:

$$\Pi = U_e + \mathbb{K} + \mathbb{P} + \mathbb{Q} \tag{25}$$

Where U_e is the total energy deformation, $\mathbb{K}$ is the kinematic energy, $\mathbb{Q}$ is the work of dissipative internal forces, and $\mathbb{P}$ is the work from the external loads, by the Principle of stationarity of the potential energy, the system will be in balance when:

$$\delta\Pi = \delta U_e + \delta\mathbb{K} + \delta\mathbb{P} + \delta\mathbb{Q} = 0 \tag{26}$$

The δU_e portion is given by the integration of the specific electric-mechanic enthalpy (or piezoelectric Gibbs' energy) over the element volume. According to Ikeda (1996), δh can be given in the e-form by:

$$\delta h = \frac{1}{2}(\delta\varepsilon \cdot \sigma - \delta E \cdot D) \tag{27}$$

Using Eq. (27) with the constitutive relations in Eq. (12), and applying the classical relations for finite element for the calculation of the $\delta\mathbb{K}$ and $\delta\mathbb{P}$ portions, found in Bathe (1996), and assuming $\delta\mathbb{Q}$ can be modeled as a linear viscous damping (with the damping matrix C), we obtain the elemental equilibrium equation:

$$\int_V \rho\delta u \cdot \delta\ddot{u} + C\delta u \cdot \delta\dot{u} + \delta\varepsilon C^E : \varepsilon - \delta\varepsilon e^t : E - \delta E e : \varepsilon - \delta E d^\varepsilon : E \, dV = \int_V \delta u \cdot b dV + \int_S \delta u \cdot t dS + \delta u \cdot F - \int_S \delta\varphi \cdot q dS - \varphi \cdot Q \tag{28}$$

Where $u = \{u_1, u_2, u_3, \theta_1, \theta_2, \theta_3\}^{n^T}, for\ n = number\ of\ nodes\ in\ the\ element$ is a vector containing each mechanical degree of freedom presented in the element, $\phi = \{\phi^n\}^T, for\ n = number\ of\ nodes\ in\ the\ element$ is a vector containing the difference of potential in each node; ρ is the density of the plate; b, t, q, F, and Q are, respectively, the body forces, surface forces, electrical charges distribution over the surface of an electrode, concentrated forces and electrical charges.

As the UEL subroutine doesn't support distributed loads, the present work uses: $b = t = q = 0$. Considering that the system of equations in Eq. (28) needs to be solved for every virtual displacement or virtual application of difference of potential, it can be written as the commonly used form:

$$\begin{aligned} M\ddot{u} + C\dot{u} + K_{uu}u + K_{u\varphi}\varphi &= F \\ K_{\varphi u}u + K_{\varphi\varphi}\varphi &= Q \end{aligned} \tag{29}$$

Where, using the Gauss Quadrature integration method the matrixes $M, C, K_{uu}, K_{u\varphi}, K_{\varphi u}\ and\ K_{\varphi\varphi}$ are given by:

$$M = \sum_{i,j=1}^{8} \rho_i \phi_{ij} \phi_{ij} \det\left(\frac{\partial x^{-1}}{\partial\zeta}\right) w_i \tag{30}$$

$$C = aM + bK_{uu} \tag{31}$$

$$K_{uu} = \sum_{i,j=1}^{8} w_i \det\left(\frac{\partial x^{-1}}{\partial\zeta}\right) \left(B_u^T \begin{bmatrix} A & B & 0 & 0 \\ B & D & 0 & 0 \\ 0 & 0 & G & G_H \\ 0 & 0 & G_H & H \end{bmatrix} B_u \right) \tag{32}$$

$$K_{u\varphi} = \sum_{i,j=1}^{8} w_i \det\left(\frac{\partial x^{-1}}{\partial\zeta}\right) \left(B_{u\varphi}^T e^T B_\varphi\right) \tag{33}$$

$$K_{u\varphi} = \sum_{i,j=1}^{8} w_i \det\left(\frac{\partial x^{-1}}{\partial \zeta}\right)\left(B_\varphi^T e B_{u\varphi}\right) \tag{34}$$

$$K_{\varphi\varphi} = \sum_{i,j=1}^{8} w_i \det\left(\frac{\partial x^{-1}}{\partial \zeta}\right)\left(B_\varphi^T d^\varepsilon B_\varphi\right) \tag{35}$$

Where w_i are the Gauss Quadrature weights and a and b are the Rayleight linear damping parameters. It should be noted that, as B_u and $B_{u\varphi}$ are matrixes that depends on the displacements, the problem is clearly non-linear. However, in such cases, the implementation in a UEL subroutine is straight-forward, as Abaqus' solver automatically updates the results using Newton's method.

4. RESULTS

The implemented model was compared, at first, to analytic results found on the literature of a planar piezoelectric beam. The first simulation is a benchmark test first proposed by Hwang and Park (1993) and analytically solved by Tzou (1993). It consists of a bimorph piezoelectric beam with dimensions of 100x5x1 mm, made of polyvinylidene fluoride (PVDF) and with properties given by Tab. 1. Comparison results between the analytic solution and the present model are given in Fig. 4.

Table 1. Material properties used in the simulations

Property	Material		
	PVDF	Carbon-epoxy laminas	Piezoelectric patches
C11 [GPa]	2,183	171,2	115,0
C12 [GPa]	0,6332	3,768	70,60
C22 [GPa]	2,183	11,08	115,0
C13 [GPa]	0,6332	3,768	109,0
C44 [GPa]	0,8463	5,4	22,00
C66 [GPa]	0,8463	5,4	12,90
e31 [C/mm²]	$3{,}266*10^{-6}$	-	$9{,}6*10^{-6}$
d33 [nF/m]	$0{,}1261*10^{-9}$	-	$0{,}171*10^{-9}$

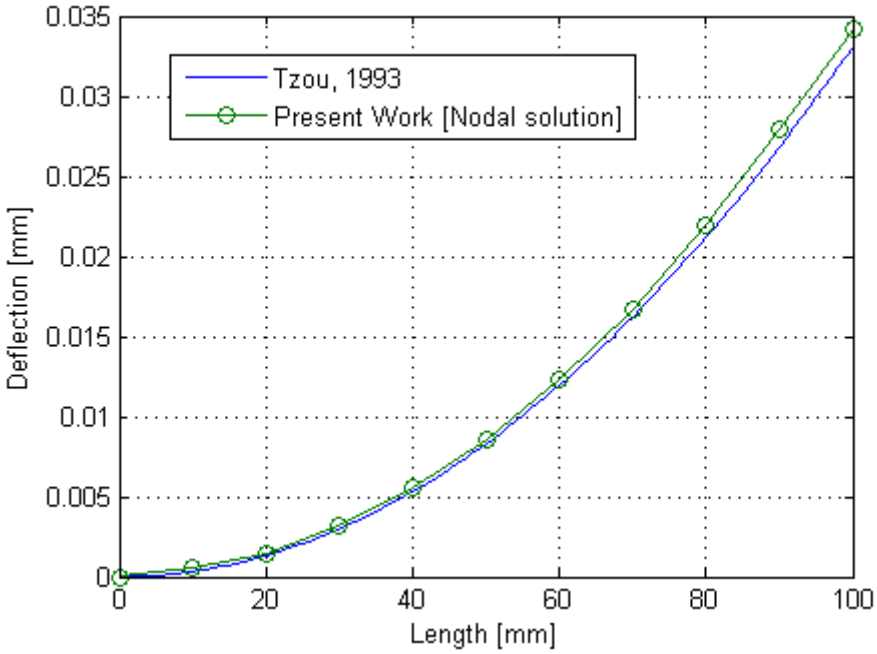

Figure 4. Results of the first example

It can be seen that the present modeling has a close result to the analytic solution, obtaining a final deflection of 3,42 mm, a 3,26% difference from Tzou (1993) solution of 3,312 mm. These differences are probably attributed to the non-linear geometrical model.

The second example, proposed by Marinković et al (2006) consists of a simple-supported composite half-cylinder with dimensions: 100 mm radius, 60 mm length and a $[0°/45°/-45°/0°]_S$ layer-up with properties given by Table 1. The

outmost layers consist of piezoelectric patches with a 0,24 mm thickness and the innermost layers consist of carbon-epoxy laminas with 0,12 mm thickness. Both a mechanical load of 100 N in the center-line and a electrical load of a 10V difference of potential were applied. A mesh consisting of 180 elements with 8 nodes each was used and is shown in Fig. 5, with the mechanical load.

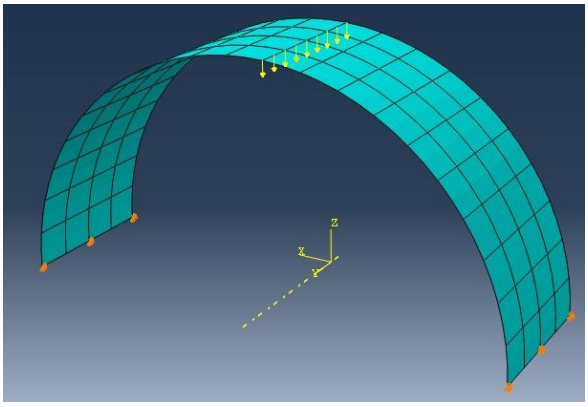

Figure 5. Mesh and mechanical load case for the second example

The deformed shapes for both the mechanical and electrical loads are shown in the Fig. 6. Results of the displacement of the centerline are shown in Fig. 7 and are compared to the results obtained by Marinković et al (2006).

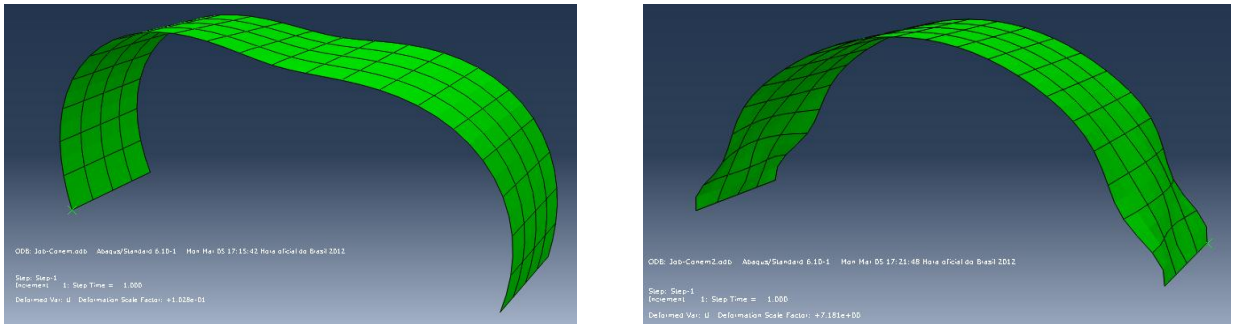

A **B**

Figure 6. Deformed shape for the: A. mechanical loads B. electrical loads

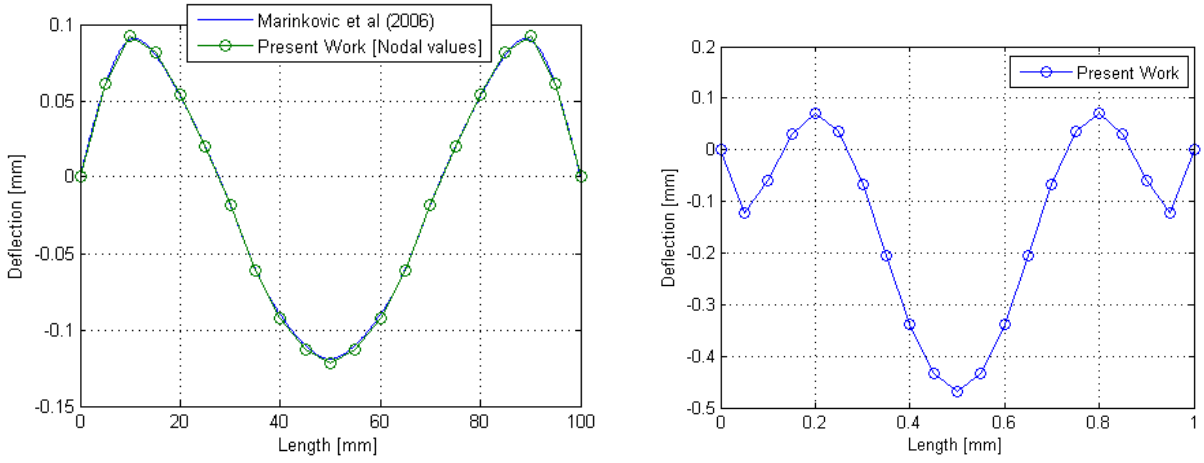

A **B**

Figure 7. Deflection of the center-line for: A. mechanical loads B. electrical loads

5. CONCLUSIONS

This work presented a co-rotational, non-linear finite element model for active composite curved plates. The model was implemented in Abaqus' UEL (User Element) subroutine and used for static simulations of numerical examples found on the literature of both planar and curved composites. The applicability of the implemented model was shown by comparing numerical simulations with results found in the literature. The results showed little differences to the ones found on the literature, probably due to the geometrical non-linear model contained in the present work. Finally, the implemented element is a base for other more complex models such dynamic and modal responses or more complex structures that will be approached in future works.

6. ACKNOWLEDGEMENTS

The authors would like to thank Research Foundation of State of Sao Paulo FAPESP (process numbers: 09/00544-5 and 10/13596-0), as well as, CNPq and FAPEMIG for partially funding the present research work through the INCT-EIE, as well as to thank CTMSP – Centro Tecnológico da Marinha – São Paulo. Finally, the authors would like to thank Prof. Reginaldo Teixeira Coelho from EESC-USP (Escola de Engenharia de São Carlos – Universidade de São Paulo) for kindly lending the licenses for the Abaqus software.

7. REFERENCES

Ahmad S., Irons B. M. and Zienkiewicz O. C., 1970, "Analysis of thick and thin shell structures by curved finite elements", Int. J. Numer. Methods Eng., vol. 2 p. 419–51

Azzouz, M. S.; Mei, C.; Bevan, J. S.; Ro, J. J.; (2001). "Finite Element Modeling of MFC/AFC Actuators and Performance of MFC", Journal of Intelligent Material Systems and Structures, vol. 12, p. 601.

Bathe, K., 1996, "Finite Element Procedures", - Prentice Hall, New Jersey.

Ikeda, T. 1996, "Fundamentals of Piezoelectricity", Oxford UniversityPress Inc., New York

Ochoa, O.O. and Reddy, 1993. "Finite Element Analysis of Composite Laminates", Kluwer Academic Publishers, Dordrecht, Boston, London.

Gabbert, U. and Marinkovic, D., 2004, "Modelling of Laminate Composites with Embedded Piezoelectric Actuators and Sensors". Mechanics, Automatic Control and Robotics, v. 4, N° 16, p. 115-120.

Marinkovic, D., Köppe H., and Gabbert, U, 2006, "Numerically Efficient Finite Element Formulation for Modeling Active Composite Laminates". Mechanics of Advanced Materials and Structures, v. 13, p 379-392.

Marinkovic, D., Köppe H., Gabbert, U, 2007, "Accurate Modeling of the Electric Field within Piezoelectric Layers for Active Composite Structures". Journal for Intelligent Material Systems and Structures, v. 18, p 503-514.

Marinkovic, D., Köppe H., Gabbert, U, 2008, "Degenerated shell element for geometrically nonlinear analysis of thin-walled piezoelectric active structures". Smart Material Structure, v. 17.

Medeiros, R.; Moreno, M. E.; Tita, V., 2010. "Electromechanical response of 1-5 piezoeletric fiber composites: a unit cell approach for numerical evaluation of effective properties.", In: VI National Congress of Mechanical Engineering – CONEM 2010.

Medeiros, R., 2012, "Desenvolvimento de uma Metodologia Computacional para Determinar Coeficientes Efetivos de Compósitos Inteligentes",(Masters Thesis), 2012, Escola de Engenharia de São Carlos, Universidade de São Paulo, São Carlos, 2003.

Paik, S. H.; Yoon, T. H.; Shin, S. J.; Kim, S. J; 2007, "Computational material characterization of active fiber composite". Journal of Intelligent Material Systems and Structures, v.18, p. 19-28.

Piefort, V, 2009, "Finite element modelling of piezoelectric active structures". (PhD. Thesis) - Faculty of Applied Sciences, Université Libre de Bruxelles.

Sartorato, M.; Tita, V.; Vera, V. R.; Tita, V., 2011, "A finite element for composite laminated beams with a shear correction factor model". In: International Congress of Mechanical Engineering COBEM, 2011, Natal. Anais do XXI COBEM.

Tzou, H.S., 1993. Piezoelectric Shells, Kluwer Academic Publishers.

8. RESPONSIBILITY NOTICE

The authors are the only responsible for the printed material included in this paper.